Journal of Molecular Catalysis B: Enzymatic 62 (2010) 173–182

Contents lists available at ScienceDirect

Journal of Molecular Catalysis B: Enzymatic

journal homepage: www.elsevier.com/locate/molcatb

# Some kinetic properties of deoxytyrosinase

J.L. Muñoz-Muñoz [a], F. García-Molina [a], P.A. García-Ruiz [b], R. Varon [c], J. Tudela [a], F. García-Cánovas [a,*], J.N. Rodríguez-López [a]

[a] *GENZ: Grupo de Investigación de Enzimología, Departamento de Bioquímica y Biología Molecular-A, Facultad de Biología, Universidad de Murcia, E-30100 Espinardo, Murcia, Spain*
[b] *QCBA: Grupo de Química de Carbohidratos y Biotecnología de Alimentos, Departamento de Química Orgánica, Facultad de Química, Universidad de Murcia, E-30100 Espinardo, Murcia, Spain*
[c] *Departamento de Química-Física, Escuela de Ingenieros Industriales de Albacete, Universidad de Castilla la Mancha, Avda, España s/n, Campus Universitario, E-02071 Albacete, Spain*

ARTICLE INFO

*Article history:*
Received 12 June 2009
Received in revised form 7 October 2009
Accepted 21 October 2009
Available online 30 October 2009

*Keywords:*
Tyrosinase
Hemocyanin
Kinetic mechanism
*deoxy*-tyrosinase
pH

ABSTRACT

Passing a nitrogen stream over a preparation of *oxy*-tyrosinase ($E_{ox}$) gives rise to the relaxed *deoxy*-tyrosinase form ($E_d^R$), which, under anaerobic conditions, slowly transforms into tense *deoxy*-tyrosinase ($E_d^T$). In the presence of oxygen, regeneration of the form $E_{ox}$ from $E_d^R$ is rapid but from $E_d^T$ it is a slow process. However, when two substrates (oxygen/*o*-diphenol or oxygen/monophenol) are simultaneously added, both the $E_d^R$ and $E_d^T$ forms rapidly revert to the active $E_{ox}$ form, pointing to a synergistic effect of both substrates. However, the activity obtained in the case of $E_d^T$ is less than that of the native enzyme and of the enzyme that can be generated rapidly by pre-incubation with oxygen of the $E_d^R$ recently formed by passage of the nitrogen stream, or that generated slowly by pre-incubating the $E_d^T$ form with oxygen. Although the $V_{max}$ of the forms $E_d^R$ and $E_d^T$ are very similar, the Michaelis constant of the latter is higher. The kinetic properties of $E_d^R$ are similar to those of the native enzyme. The behaviour of the monophenols is similar to that of the *o*-diphenols, although, while the latter inactivate the enzyme under anaerobic conditions, the former protect it from inactivation. The pH affects the transition from $E_d^R$ to $E_d^T$, which is more rapid at pH 6.5, at which value the kinetic properties of the native enzyme and of $E_d^T$ are similar and the oxygenation step in which $E_d^T$ regenerates $E_{ox}$ is more rapid. At pH values other than 6.5, the transition of $E_d^R$ to $E_d^T$ takes place slowly. From a study of the effect of pH on the transition of $E_d^R$ to $E_d^T$ and of the re-oxygenation of $E_d^T$ to $E_{ox}$, the possible existence of two apparent p$K_a$s, with approximate values of 6.0 and 6.8, may be surmised. At high pH, the enzyme contains two acid/base groups carrying negative charges, which repel (pH > 6.8) or two positive charges (at pH < 6.0), which also repel, while at ~pH 6.5 one positive and one negative group exists, which prevents the separation of the two copper atoms.



## 1. Introduction

Tyrosinase (EC 1.14.18.1) is involved in melanin biosynthesis in bacteria, plants and mammals. The enzyme catalyses the ortho-hydroxylation of monophenols (monophenolase activity) and the oxidation of *o*-diphenols to *o*-quinones (diphenolase activity). The catalytic centre of tyrosinase possesses a binuclear copper similar to that of hemocyanin and catechol oxidase [1,2]. The catalytic cycle of tyrosinase has three enzymatic forms: $E_m$ (*met*-tyrosinase), with the copper as $Cu^{2+}Cu^{2+}$, $E_d$ (*deoxy*-tyrosinase), with the copper as $Cu^{+}Cu^{+}$ and $E_{ox}$ (*oxy*-tyrosinase) with copper in the form $Cu^{2+}Cu^{2+}O_2^{2-}$ [3].

The three proteins with type 3 active copper centres which take part in $O_2$ binding and activation are hemocyanin, which binds $O_2$ reversibly, catechol oxidase, which converts catechols to the corresponding *o*-quinones, and tyrosinase, which hydroxylates monophenols and converts catechols to *o*-quinones [1,2]. In the structures of hemocyanin [4], catechol oxidase [5] and tyrosinase from *Streptomyces castaneoglobisporus* [6], each copper ion is coordinated by three histidines. Of the three proteins described, the binding of oxygen to the *deoxy* form has mainly been studied in *deoxy*-hemocyanin [7–12]. Some properties of the *deoxy* form of tyrosinase from *Streptomyces glaucencens* and *Neurospora crassa* have been studied [13], as well as the oxygen binding in tyrosinases from *Streptomyces antibioticus* [14] and *Agaricus bisporus* [15]. Subsequently, comparative studies were made of the three related proteins, hemocyanin, catechol oxidase and tyrosinase [2,10,16–18], while hemocyanin activity on *o*-diphenols [19–26] and on monophenols [27] has been demonstrated. Furthermore, synthetic copper complexes show-

* Corresponding author. Fax: +34 968 364147.
*E-mail address:* canovasf@um.es (F. García-Cánovas).
*URL:* http://www.um.es/genz (F. García-Cánovas).

1381-1177/$ – see front matter © 2009 Elsevier B.V. All rights reserved.
doi:10.1016/j.molcatb.2009.10.005

ing activity on *o*-diphenols and monophenols have been described [28–30].

In our studies of the kinetic mechanism of tyrosinase [31–34], especially of the suicide inactivation processes with phenolic compounds [35] and with ascorbic acid [36], we proposed an action mechanism on monophenols and *o*-diphenols and worked with tyrosinase in the different forms existing in the catalytic cycle: $E_m$, *met*-tyrosinase; $E_{ox}$, *oxy*-tyrosinase and $E_d$, *deoxy*-tyrosinase [36].

Mason's study of mushroom tyrosinase [3] demonstrated that when a nitrogen stream is passed through a solution of $E_{ox}$, the typical spectrum of $E_{ox}$ disappears and that when attempts are made to regenerate the enzyme after a certain time, only 50–60% is recovered, suggesting that the enzyme evolves towards a form that is re-oxygenated slowly.

To broaden our knowledge of the different enzymatic forms of tyrosinase, we have made a kinetic study of the evolution of $E_d$ under anaerobic conditions and of the kinetic of the re-oxygenation process. We have further studied the effect of the order in which the substrates (oxygen/*o*-diphenol or oxygen/monophenol) are added to the enzyme, considering the effect of pH on the transition of $E_d$ and on its re-oxygenation, and discussed the possibility that two apparent p$K_a$s may be responsible for its transition. The results are discussed in relation with the process described for the oxygenation of *deoxy*-hemocyanin [8].

## 2. Experimental

### 2.1. Materials

Mushroom tyrosinase or polyphenol oxidase (PPO; *o*-diphenol:$O_2$ oxidoreductase, EC 1.14.18.1, 8300 units/mg), was supplied by Sigma (St. Louis, MO). Tyrosinase was purified as previously described [32]. The protein concentration was determined by Bradford's method [37] and using bovine serum albumin as the standard. The substrates used were: hydrogen peroxide, supplied by Scharlau (Madrid, Spain), 4-*tert*-butylcatechol (TBC) supplied by Acros Co. (Madrid, Spain), and L-tyrosine and L-dopa supplied by Aldrich (Switzerland). Other chemicals were of analytical grade and supplied by Merck (Darmstadt, Germany).

### 2.2. Methods

#### 2.2.1. Oxymetric assays

Measurements of dissolved oxygen concentration were made with a Hansatech (Kings Lynn, Cambs, UK) oxygraph unit controlled by a PC-computer. The oxygraph used a Clark-type silver/platinum electrode with a 12.5 μm Teflon membrane. The sample was continuously stirred during the experiments and its temperature was maintained at 25 °C. The zero oxygen level for calibration and experiments was obtained by bubbling oxygen-free nitrogen through the sample for at least 10 min. The oxygraph was calibrated as described in [38].

#### 2.2.2. Spectrophotometric assays

When the substrate was TBC, the reaction was followed by monitoring the formation of *o*-*tert*-butylquinone at 410 nm ($\varepsilon$ = 1200 $M^{-1}$ $cm^{-1}$) [39]. When the substrate was L-tyrosine or L-dopa the increase in absorbance at 475 nm ($\varepsilon$ = 3500 $M^{-1}$ $cm^{-1}$) was followed [39].

#### 2.2.3. Generation of $E_{ox}$ and $E_d$

$E_{ox}$ was generated from the native enzyme, adding micromolar concentrations (5 μM) of $H_2O_2$ so that the $E_m$ form passed to $E_{ox}$. $E_d$ was generated by bubbling nitrogen through the $E_{ox}$ solution to transform all the $E_{ox}$ to $E_d$ ($E_{ox} \rightleftarrows E_d + O_2$) [36,40].

#### 2.2.4. Evaluation of enzymatic species $E_m$, $E_d$ and $E_{ox}$ in an enzymatic preparation of tyrosinase

Regardless of the source, tyrosinase preparations are reported to contain three enzyme forms, namely $E_m$, $E_d$ and $E_{ox}$ [40]. To evaluate these enzymatic forms in an enzyme sample, we propose a kinetic method [36] based on the fact that the inactivation of these forms by 2-mercaptoethanol [41] occurs over a wide time range: inactivation constants of 0.014, $4 \times 10^{-5}$ and $1 \times 10^{-5}$ $s^{-1}$ for $E_{ox}$, $E_m$ and $E_d$, respectively. Under aerobic conditions at oxygen concentrations of 0.26 mM, practically the only forms existing are $E_{ox}$ and $E_m$ [32]. Note that the difference between $k_i^{ox}$ and $k_i^m$ is three orders of magnitude, a difference that can be used to evaluate these enzymatic forms.

The experimental method consists of pre-incubating the enzyme under aerobic conditions with 2-mercaptoethanol at a concentration of 10 μM. Aliquots of the reaction mixture are taken at different incubation times and immediately assayed for residual activity using TBC as the substrate. In this way, at sufficiently long times, a situation is reached in which the activity tends asymptotically to a constant value. The decrease in the initial activity to reach this approximately constant final value would correspond to the concentration of $E_{ox}$ in the medium. In this way, inactivation assays of the enzyme sample previously incubated with different concentrations of $H_2O_2$ in the μM order are made with 2-mercaptoethanol. This gives rise to different concentrations of $E_{ox}$ and therefore different levels of activity in the linear zone [36].

Analysis by non-linear regression fitting of the experimental data to the uniexponential equation:

$$\frac{A_t}{A_0} = \frac{A_{m_0}}{A_0} + \frac{A_{ox_0}}{A_0} e^{-k_{app}^{ox} t} \quad (1)$$

gives the values of $(A_{m_0}/A_0) \times 100$, which is the percentage of $E_m$, $(A_{ox_0}/A_0) \times 100$ which is the percentage of $E_{ox}$ and $k_{app}^{ox}$, the apparent inactivation constant. In Eq. (1), $A_t$, is the residual activity at time $t$, $A_0$ is the initial activity, $A_{m_0}$ is the activity corresponding to $E_{m_0}$ and $A_{ox_0}$ is the activity corresponding to $E_{ox_0}$ [36].

The representation of the decrease in activity (corresponding to $E_{ox}$) *vs.* instantaneous activities, when $t \rightarrow \infty$, (corresponding to $E_m$) shows a linear variation, which can be used as a calibration straight to determine the percentages of $E_{ox}$ and $E_m$ in an enzymatic preparation of tyrosinase.

#### 2.2.5. Characterisation of the kinetic parameters of the native enzyme, $E_d^R$ and $E_d^T$

The kinetic parameters $V_{max}^D$ and $K_m^D$ for the diphenolase activity were calculated from the initial velocities, $V_0^D$, with TBC and $O_2$ (0.26 mM) as substrates [39]. These values were fitted to the Michaelis equation by non-linear regression [42]. At pH 7.0, since the $E_d^R$ form evolves slowly to $E_d^T$ at 25 °C, the native enzyme (without passing nitrogen) and the forms $E_d^R$ and $E_d^T$ were maintained in an ice bath, while the measurements with $E_d^R$ were made immediately in order to delay the transition. In the same way, at pH 6.5, the native form and $E_d^T$ were analysed for the diphenolase activity on TBC.

The kinetic parameters, $V_{max}^M$ and $K_m^M$, for the monophenolase activity were calculated from the initial velocities, $V_0^M$, using L-tyrosine and adding an amount of L-dopa so that $[D]_{ss}/[M]_{ss} = 0.035$ [43] and recording the increase in absorbance at 475 nm. At pH 7.0, using the same methodology as for the diphenolase activity, the native enzyme and the forms $E_d^R$ and $E_d^T$ were characterised. In the same way, at pH 6.5, the native form and $E_d^T$ were analysed using L-tyrosine as substrate.

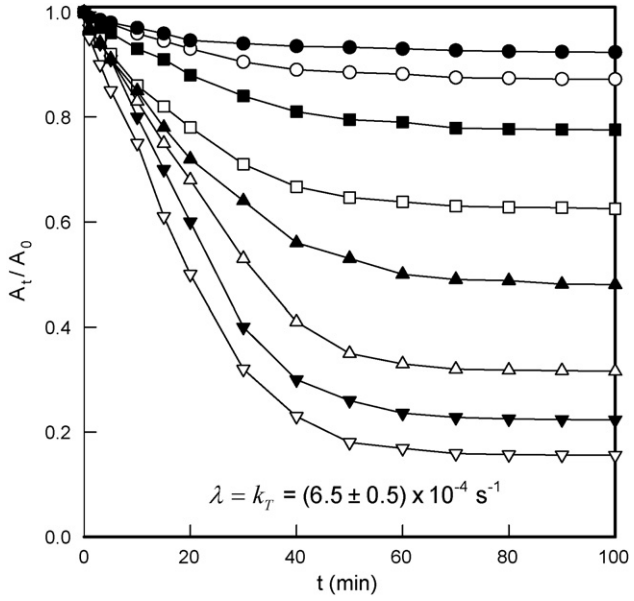


**Fig. 1.** Variation of the $A_t/A_0$-values *vs.* time obtained from a kinetic study of transition of $E_d^R$ to $E_d^T$ followed through the diphenolase activity. The experimental conditions were as follows: 30 mM sodium phosphate buffer (pH 7.0), 25 °C. A nitrogen stream was first passed through the buffer and then 10 nM enzyme (previously treated with 5 μM $H_2O_2$) was added; still passing the nitrogen stream, aliquots were taken at the indicated times and the activity was followed using different concentrations of TBC, measuring the increase in absorbance at λ = 410 nm. TBC concentrations (mM) were: ▽ 0.5, ▼ 1, △ 2, ▲ 4, □ 5, ■ 7, ○ 9 and ● 15.

### 2.2.6. Kinetic study of the transition of $E_d^R$ to $E_d^T$

The data of this transition were fitted to the equation (see Appendix A):

$$\frac{A_t}{A_0} = \alpha + \beta e^{-\lambda t} \quad (2)$$

where $A_t$ is the instantaneous activity, $A_0$ is the instantaneous activity at $t = 0$, and $\lambda = k_T$, the apparent transition constant. The parameters $\alpha$ and $\beta$ are functions of the substrate concentration (see Appendix A). Fitting the data shown in Fig. 1 to Eq. (2) by non-linear regression provides the value of the transition constant, $k_T = (6.5 \pm 0.5) \times 10^{-4}\ s^{-1}$. Note that when $t \to \infty$, $A_\infty/A_0 = \alpha$, and the amplitude of the exponential is $(A_0 - A_\infty)/A_0 = 1 - \alpha = \beta$.

### 2.2.7. Inactivation of $E_d^R$ and $E_d^T$ by o-diphenols

All the native enzyme was converted into $E_{ox}$ by adding $H_2O_2$ (2 μM). A nitrogen stream was then passed to obtain $E_d^R$. The form $E_d^R$ was incubated with L-dopa (5–45 μM), and aliquots were taken at different times to measure instantaneous activities using L-dopa.

Once $E_d^R$ had been generated, 90 min were allowed to pass for it to be transformed into $E_d^T$. This form was then incubated with L-dopa (5–45 μM), and aliquots were taken at different times to measure instantaneous activities using L-dopa.

### 2.2.8. Effect of monophenols on enzyme inactivation by o-diphenols

The forms $E_d^R$ or $E_d^T$ were pre-incubated with L-tyrosine (20 μM) and in the presence of L-dopa (5–45 μM), while aliquots were taken at different times to measure instantaneous activities using L-dopa.

## 3. Results and discussion

Tyrosinase, in its native state, basically exists in three forms known as *met*-tyrosinase ($E_m$), *deoxy*-tyrosinase ($E_d$) and *oxy*-tyrosinase ($E_{ox}$) [40]. As described in Section 2, the addition of $H_2O_2$ (μM) to an aerobic medium transforms the $E_m$ into $E_{ox}$ [3]. Passing a stream of nitrogen transforms $E_{ox}$ into $E_d$. This $E_d$, with time, evolves towards another enzyme form with different kinetic properties (higher $K_m$ for substrates and slightly lower $V_{max}$). This transition, therefore, can be followed from the loss of enzymatic activity with time at a non-saturating substrate concentration. By analogy with the nomenclature used by Solomon for *deoxy*-hemocyanin [8], these enzymatic forms could be regarded as $E_d^R$ and $E_d^T$, R (relaxed) and T (tense), and, in the case of *deoxy*-hemocyanin, the distances between the copper atoms at the active site are 3.5 Å (R) and 4.6 Å (T), respectively [8].

**Table 1**
Kinetic constants of the native, $E_d^R$ and $E_d^T$ forms of tyrosinase.

| | $K_m^D$(mM) | $V_{max}^D$(μM/s) | $K_m^M$(mM) | $V_{max}^M$(μM/s) |
|---|---|---|---|---|
| $E_{native}$ | 1.39 ± 0.14[a] | 37.11 ± 0.74[a] | 0.17 ± 0.02[b] | 0.52 ± 0.02[b] |
| $E_d^R$ | 1.80 ± 0.19[a] | 36.19 ± 0.96[a] | 0.19 ± 0.02[b] | 0.48 ± 0.02[b] |
| $E_d^T$ | 3.21 ± 0.38[a] | 33.28 ± 0.99[a] | 0.40 ± 0.04[b] | 0.45 ± 0.01[b] |
| $E_{native}$ | 2.12 ± 0.24[c] | 37.21 ± 1.45[c] | 0.29 ± 0.01[d] | 0.53 ± 0.03[d] |
| $E_d^T$ | 2.21 ± 0.28[c] | 37.08 ± 1.92[c] | 0.31 ± 0.01[d] | 0.54 ± 0.03[d] |

$K_m^D$ = Michaelis constant for *o*-diphenol (TBC). $V_{max}^D$ = Maximum rate for *o*-diphenol (TBC). $K_m^M$ = Michaelis constant for monophenol (L-tyrosine). $V_{max}^M$ = Maximum rate for monophenol (L-tyrosine).

[a] Determined in 30 mM sodium phosphate buffer (pH 7.0) and using TBC as substrate. The enzyme concentration was 30 nM.

[b] Determined in 30 mM sodium phosphate buffer (pH 7.0) and using L-tyrosine as substrate and L-dopa with ratio constant of 0.035. The enzyme concentration was 75 nM.

[c] Determined in 30 mM sodium phosphate buffer (pH 6.5) and using TBC as substrate. The enzyme concentration was 30 nM.

[d] Determined in 30 mM sodium phosphate buffer (pH 6.5) and using L-tyrosine as substrate and L-dopa with ratio constant of 0.035. The enzyme concentration was 75 nM.

### 3.1. Diphenolase activity

### 3.1.1. Kinetic study of transition of $E_d^R$ to $E_d^T$

The native enzyme and the forms $E_d^R$ and $E_d^T$ are characterised kinetically by the kinetic constants and parameters shown in Table 1 (see Section 2). The kinetic parameters shown in this table indicate that the enzyme form $E_d^T$ has the highest $K_m$, that is, a lower affinity for the *o*-diphenol, but, the $V_{max}$ for all these forms are the same. As regards $E_d^R$, since this form is not totally stable, it may partially evolve towards $E_d^T$. Note that the kinetic behaviour of these enzymatic forms as regards $V_{max}$ and $K_m$ is similar to that shown by the native enzyme with respect to the Dopa isomers, other enantiomers [44] and, in general, all *o*-diphenols [45]. In all these cases, it can be seen that the catalysis is associated with the nucleophilic power of the oxygen of the OH in *para*-position of the *o*-diphenol. Since, in this work, the *o*-diphenol is always TBC ($\delta_4$- and $\delta_3$-values of 144.09 and 146.24 ppm, respectively [45]), the $V_{max}$-value might be very similar. Bearing in mind the increase in $K_m$ in the form $E_d^T$, the difference in the initial velocities at a non-saturating substrate concentration permits us to follow the transition. Fig. 1 shows the relative values of the initial velocities, revealed with TBC with respect to the transition time.

### 3.1.2. Kinetic of $E_d^T$ re-oxygenation

These experiments study the transformation of $E_d^T$ to $E_{ox}$, for which the most straightforward kinetic scheme would be (Schemes 1A and 1BSM):

$$E_d^T + O_2 \underset{k_r}{\overset{k_b}{\rightleftharpoons}} E_d^T O_2 \xrightarrow{k^*} (E_d^T O_2)^* \xrightarrow{k_{ox}} E_{ox}$$

**Scheme 1A.** Kinetic mechanism of the oxygenation of the form $E_d^T$.

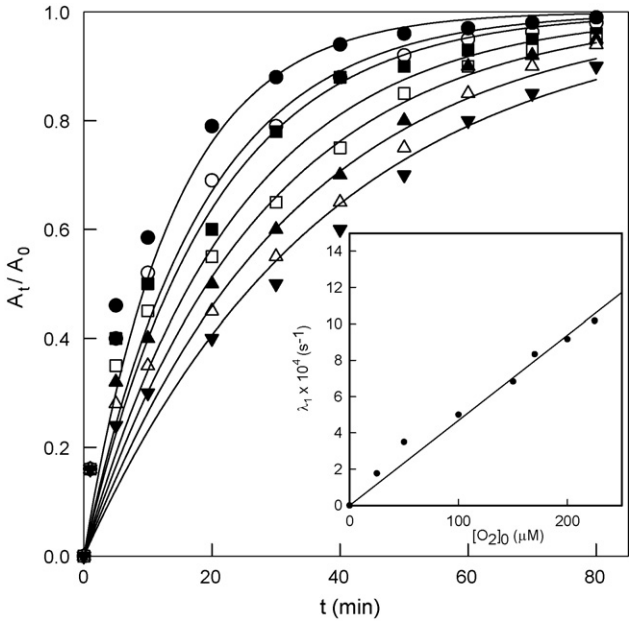


**Fig. 2.** Dependence of the $A_t/A_0$-values *vs.* time obtained from a kinetic study of oxygenation of $E_d^T$. A nitrogen stream was first passed through 30 mM sodium phosphate buffer (pH 7.0), 25 °C. Then, 10 nM of the $E_{ox}$ form was added; still passing the nitrogen stream, the mixture was left for 90 min for the $E_d^R$ to be transformed into $E_d^T$. The enzyme, in the form of $E_d^T$, was added to the cell of the oxygraph containing 30 mM sodium phosphate buffer (pH 7.0) at 25 °C, and a sufficient concentration of oxygen so that the final $O_2$ concentrations (μM) become: ▼ 25, △ 50, ▲ 100, □ 150, ■ 175, ○ 200 and ● 225. At the indicated times, 100 μl of the above mixture was extracted with microsyringe and added to the reaction cell with $O_2$ (0.26 mM) and TBC (1 mM). Inset: Representation of the apparent transition constant $\lambda_1$ *vs.* $[O_2]_0$, the initial oxygen concentration.

The incubation of $E_d^T$ is started at different concentrations of oxygen. Aliquots are taken at different times and the enzymatic activity is revealed with TBC (see Fig. 2). Note the monoexponential behaviour, which depends on the concentration of $O_2$. The kinetic analysis of the mechanism depicted in Scheme 1A (see Appendix B) indicates that $E_{ox}$ is accumulated with time according to:

$$[E_{ox}] = [E_d^T]_0(1 - e^{-\lambda_1 t}) \quad (3)$$

where $\lambda_1$ represents the apparent constant of $E_d^T$ oxygenation and the analytical expression of $\lambda_1$ is:

$$\lambda_1 = \frac{k^*[O_2]_0}{K_{O_2}^T + [O_2]_0} \quad (4)$$

with

$$K_{O_2}^T = \frac{k_r}{k_b} \quad (5)$$

Analysis by non-linear regression of the velocities with time, according to Eq. (3), provides the apparent transition constant $\lambda_1$. The representation of $\lambda_1$ *vs.* $[O_2]_0$, Fig. 2 Inset, does not show a hyperbolic behaviour, indicating that the value of $K_{O_2}^T$ for $E_d^T$ is higher than for the native enzyme, so that $E_d^T$ cannot be saturated at the oxygen concentrations used. There is an apparent contradiction between the initial velocity experiments, which give the results shown in Table 1, and those shown in Fig. 2. In the former, an aliquot of $E_d^T$ shows its activity as soon as it comes into contact with the substrates $O_2$/*o*-diphenol together, while in Fig. 2, where $E_d^T$ is pre-incubated with oxygen, only a small part of the activity is detected, although at long time intervals, all the activity is revealed (as in the case of the native enzyme). These experiments can be explained by a similar mechanism to that proposed by Solomon [8] (Scheme 1BSM) for the oxygenation of *deoxy*-hemocyanin. According to the mechanism proposed in [8], the substrate ($O_2$) approaches the binuclear copper (I) site driven by optimizing the metal–ligand overlap, while the binuclear pathway for the binding of $O_2$ is favoured energetically to the mononuclear pathway and the changes in the charge density of the coppers and oxygens are similar, indicating that this is a simultaneous two electron-transfer process, that is, there is a charge transfer step [8]. Subsequently, the singlet state is preferred to the triplet state [8]. Furthermore, in [8] it is proposed that *deoxy*-hemocyanin in the form T [$d(Cu^A - Cu^B) = 4.6$ Å] is less energetic (15.6 kcal/mol) and therefore more stable than R [$d(Cu^A - Cu^B) = 3.5$ Å] (17.8 kcal/mol); but, whatever the case, the formation of the oxy form is exothermic and for hemocyanin the value of $\Delta G$ determined from experimental data is negative, while at the end of the process, all the protein is in the form of *oxy*-hemocyanin [8].

In the case of tyrosinase, the data obtained suggest that a similar process might occur. The diminution in the affinity (increased $K_m$ for *o*-diphenol and oxygen) might be explained by the fact that under anaerobic conditions the $E_d^R \rightarrow E_d^T$ transition would involve separation of the copper atoms and the forms $E_d^R$ and $E_d^T$ would be similar to the forms R and T described for *deoxy*-hemocyanin [8]. Incubation of $E_d^T$ with $O_2$ triggers the slow process described above (Scheme 1BSM), culminating in the formation of $E_{ox}$, which has recovered all its activity on *o*-diphenol. In this case, the *o*-diphenol binds in the same way as it does to the native enzyme, transferring the proton of the OH in *para*-position to the peroxide, which acts as a base, while the resulting anion attacks $Cu^B$ of the active site and then the OH in *meta*-position would transfer its proton to the histidine 54 ($His^{54}$) of the $Cu^A$ [6]. The $His^{54}$ is released, and the *o*-diphenol binds diaxially, leading to a joint oxidation/reduction step as a result of the coplanarity of the orbitals and an activity similar to that of the native enzyme. However, as Fig. 2 shows, once this process has started, only the activity of the $E_{ox}$ generated (Scheme 1BSM) will be detected. But note that the measurements of initial velocity in the presence of $O_2$ and *o*-diphenol point to a synergic effect, so that the presence of the *o*-diphenol will immediately re-establish the $O_2$ bond. This form, which is recovered in a way that differs from that described in [8], shows worse kinetic constants (especially $K_m$) than the native form and also than $E_d^R$ (see Table 1) (Scheme 1CSM). Similarly, the form $E_d^R$, when brought into contact simultaneously with the *o*-diphenol/$O_2$, shows immediate enzymatic activity—almost the same as that shown by the native enzyme but greater that that of $E_d^T$. When both forms $E_d^R$ and $E_d^T$ come into simultaneous contact with the oxygen/*o*-diphenol, the form $E_{ox}D$ may be generated in a different way, especially in the case of $E_d^T$, when the *o*-diphenol cannot transfer the proton of OH in *para*-position to the peroxide, since it does not exist. In this case, it may first transfer the proton to the $His^{54}$, the phenolate binding to $Cu^A$. The copper atoms restructure and bind with the $O_2$, while the proton of the OH in *meta*-position is transferred to the peroxide, which would act as a base, and the phenolate can now bind to the $Cu^B$.

This atypical generation of $E_{ox}D$ may reduce the enzymatic activity, as occurs experimentally, and is lower for $E_d^T$ than for $E_d^R$. Although activity is obtained, the enzyme in the form $E_d^T$ does not recover its native form in a few turnovers, since no lag period appears in the kinetic measurements. However, as described in Schemes 1CSM and 1DSM, the alternative mechanism proposed for $E_d^T$ (Scheme 1CSM) is also possible. The influence of the oxygen concentration during pre-incubation is clear in the results shown in Fig. 3, as the oxygen concentration in the reaction medium increases, so the enzyme activity increases, but note that this effect does not occur at $t \rightarrow 0$, since $E_d^R$, recently formed, is rapidly oxygenated as it passes to $E_{ox}$ since its $K_m^{O_2}$ is low (Scheme 1DSM).

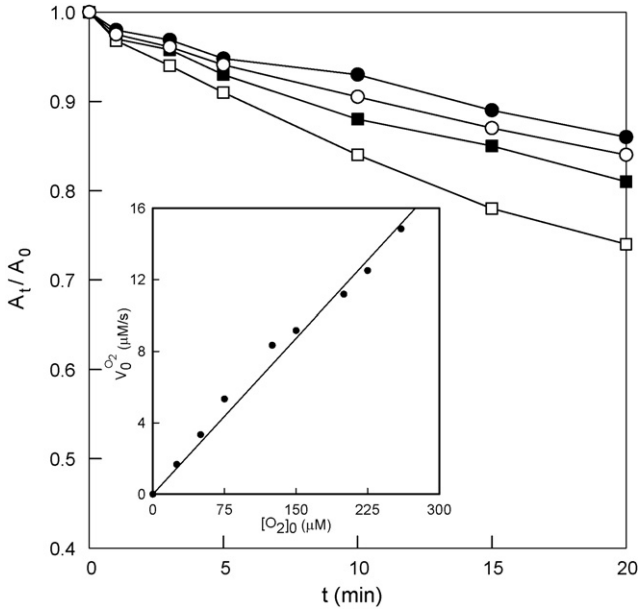


**Fig. 3.** Effect of oxygen concentration on the $A_t/A_0$-values in following the transition of $E_d^R$ to $E_d^T$. The experimental conditions were 30 mM sodium phosphate buffer (pH 7.0), 25 °C (previously de-aired with $N_2$). The enzyme $E_{ox}$ is transformed into $E_d^R$ under the nitrogen while the transition to $E_d^T$ is studied under a continuous nitrogen stream. Aliquots are revealed in media with TBC (1 mM) and different initial oxygen concentrations (μM): without previous pre-incubation, □ TBC + $O_2$ (260 μM) at the same time; with previous pre-incubations (1 min) with oxygen at the following initial concentration (μM): ■ 130, ○ 195 and ● 260 and finally the reaction is started with TBC (1 mM). Inset: representation of initial rates of oxygen consumption, $V_0^{O_2}$ *vs.* $[O_2]_0$, the initial oxygen concentration, for the enzymatic form $E_d^T$.

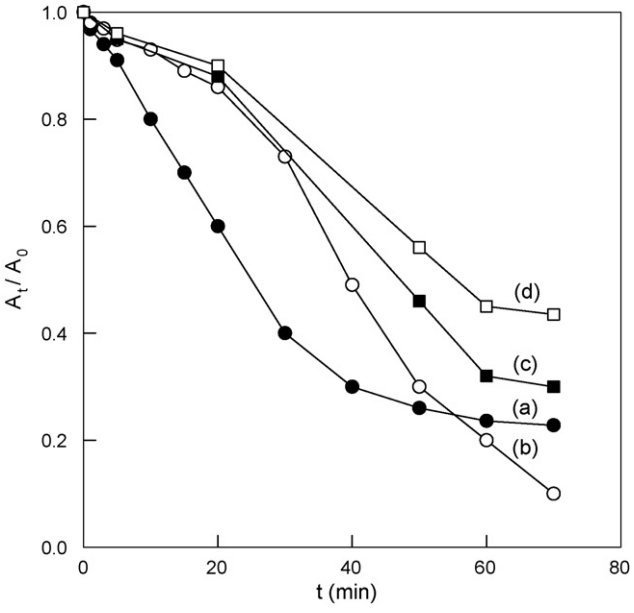


**Fig. 4.** Variation of the $A_t/A_0$-values *vs.* time obtained from a kinetic study of the effect of pre-incubation time with oxygen on transition of $E_d^R$ to $E_d^T$. The experimental conditions were: 30 mM sodium phosphate buffer (pH 7.0), 25 °C de-aired with $N_2$. The enzyme $E_{ox}$ (10 nM) was then added under a continuous nitrogen stream. At the times indicated in the figure, aliquots were taken and added to the cell containing phosphate buffer pH 7.0 and oxygen. The mixture was left to incubate, starting the reaction with TBC (1 mM) and measuring the initial velocity at λ = 410 nm. ● Without pre-incubation with $O_2$ [curve (a)]. Pre-incubating with $O_2$ (260 μM) during; ○ 1 min [curve (b)], ■ 5 min [curve (c)] and □ 15 min [curve (d)].

At longer times, much of the $E_d^R$ has been transformed into $E_d^T$ and this new form has less affinity for oxygen, that is, a higher $K_m^{O_2}$ (Schemes 1BSM and 1CSM). Fig. 3 Inset shows how the enzyme in the form $E_d^T$, at saturating TBC concentrations, is not saturated by the concentrations of oxygen used.

### 3.1.3. Study of the transition of $E_d^R$ to $E_d^T$ with the sequential addition of the substrates, $O_2$ and *o*-diphenol

The effect of the oxygen concentration on the kinetic of the transformation of $E_d^T$ into $E_{ox}$ is shown in Fig. 2 and its effect on the apparent delay in the transition of $E_d^R$ into $E_d^T$ is depicted in Fig. 3. In Fig. 4, we depict the effect of the pre-incubation time of an aliquot of the enzyme at a fixed concentration of oxygen on the transition of $E_d^R$ into $E_d^T$. As can be seen, the order in which the substrates are added affects this process and this helps confirm the validity of Schemes 1A, 1BSM, 1CSM and 1DSM proposed to explain the transition of $E_d^R$ to $E_d^T$ and $E_d^T$ to $E_{ox}$.

The experiment consisted of studying the transition of $E_d^R$ to $E_d^T$ under anaerobic conditions, but treating the aliquot obtained of the enzyme with $O_2$ for different pre-incubation times (0, 1, 5 and 15 min, respectively), and beginning the reaction with *o*-diphenol.

Curve (a) of Fig. 4 corresponds to the transition of $E_d^R$ to $E_d^T$, determining the activity of the aliquot obtained with the simultaneous addition of the substrates $O_2$/*o*-diphenol. In this curve one must obviously bear in mind the exact moment at which the aliquot is taken. At short times, for example, the enzyme would be in the form $E_d^R$ and Scheme 1DSM would explain the recovery of the enzymatic activity. However, at long times, the enzyme would be like $E_d^T$ Scheme 1CSM would basically explain the activity. Curves (b), (c) and (d) are obtained by following the transition ($E_d^R$ to $E_d^T$), treating the aliquot obtained with the same oxygen concentration but pre-incubating for different times. Once again, we must bear in mind the times at which the aliquot is taken and its behaviour. Note that at short times there are practically no differences in the enzymatic activity obtained in any of the cases. Hence, Scheme 1DSM would explain all the cases, the enzyme being practically the same as $E_d^R$. However, at longer timer of the transition, the effects of the pre-incubation time with oxygen become patent in the transition of $E_d^R$ to $E_d^T$. At very short pre-incubation times (1 min), Fig. 4 curve (b), the representation of Scheme 1ESM would explain the experimental results: the enzyme is not transformed into $E_{ox}$, the substrate (*o*-diphenol) has no synergic effect and the enzymatic activity is very low [Fig. 4 curve (b)]. In curves (c) and (d) of Fig. 4, the importance of the pre-incubation time is evident, and can be explained according to Scheme 1BSM. At longer pre-incubation times, there is already some $E_{ox}$ and so more enzymatic activity is obtained [Fig. 4, curves (c) and (d)].

The slow stages proposed in these schemes for the re-oxygenation of $E_d^T$ may explain the experimental results described in [3], in which, after passing a nitrogen stream, the total spectrum of the *oxy*-tyrosinase form is not recovered [3].

### 3.1.4. Effect of pH on transition of $E_d^R$ to $E_d^T$

The results of studying the effect of pH on the kinetic of the transition of $E_d^R$ to $E_d^T$ are shown in Fig. 5. The value of the apparent transition constant, $k^{app}$, remains practically constant at very acidic pH values, reaches a maximum at pH 6.5 and then declines at higher pHs (Fig. 5 Inset). However, the amplitude of the exponential (Fig. 5 Inset) decreases as the pH rises, with a minimum at 6.5 and increasing at higher values. These findings suggest the existence of two significant apparent p$K_a$s for this transition, one corresponding to pH ≈ 6.75 and the other to pH ≈ 6.0. The pH optimum for this transition is 6.5, as seen from Fig. 5 Inset, in which the kinetic properties of $E_d^T$ are very similar to those of the native enzyme (Table 1). A qualitative explanation could be that outlined in the following schemes:

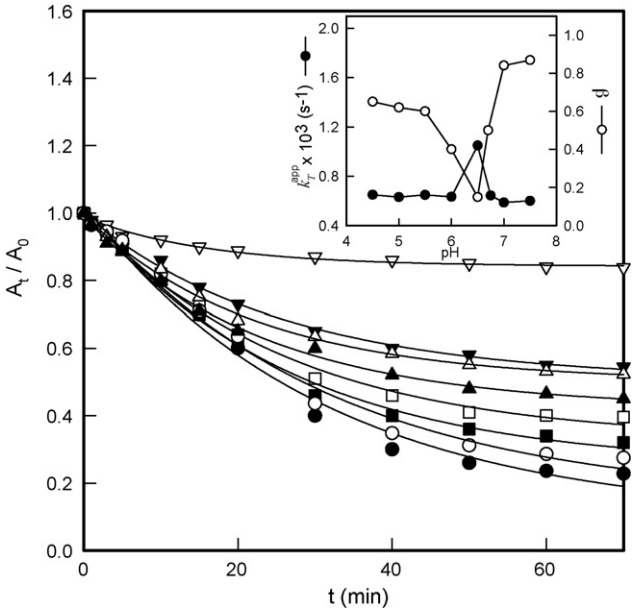


**Fig. 5.** Dependence of the $A_t/A_0$-values *vs.* time obtained from a kinetic study of the effect of pH on the transition of $E_d^R$ to $E_d^T$. The form $E_d^R$ was generated as in Fig. 1 at each pH, and the transition in a nitrogen atmosphere was studied by taking aliquots at the indicated times and revealed with TBC (1 mM). The buffers used (previously deaired with $N_2$) were 30 mM sodium acetate buffer (pH 4.0–5.5) and 30 mM sodium phosphate buffer (pH 6.0–7.5), 25 °C. The pH values were: ● 7.5, ○ 7.0, ■ 6.75, ▽ 6.5, □ 6.0, ▲ 5.5, ▼ 5.0 and △ 4.5. Inset: Representation of $k_T^{app}$ *vs.* pH (♦) and $\beta$ *vs.* pH (◊).

At pH values > 6.5, the form $E_d^R$ could have two negative charges that repel each other and the enzyme would evolve slowly towards $E_d^T$, while the two copper atoms of the active site are more separate [8]. At pH values < 6.5, the form $E_d^R$ would have two positive charges that again repel each other as the transition to $E_d^T$ continues. Furthermore, the values of the apparent transition constant are practically identical (Fig. 5 Inset). At pH 6.5, the enzyme would be as described in Scheme 2A, with a positive and negative charge. The attraction between these charges would prevent the transition to $E_d^T$ from being so great, as occurs at both high and low pH values. In this way, the kinetic constants of the different enzymatic forms (native and $E_d^T$) are practically the same at pH 6.5, that is, the copper atoms hardly separate. This hypothesis could be supported by the findings of the existence of a salt bridge between two helices that is conserved in hemocyanin, catechol oxidase and tyrosinase between Arg(Lys)-Asp, as has been described previously [46].

### 3.1.5. *Effect of pH on re-oxygenation of $E_d^T$*

The form $E_d^T$ was generated in 1 mM sodium phosphate buffer pH 7.0 as described in Section 2. The enzyme was then introduced in the oxygraph cell at different values of pH and with a 30 mM buffer. The re-oxygenation process was followed by taking aliquots at different times. As described previously, the oxygenation kinetic of $E_d^T$ at pH 7.0 showed monoexponential behaviour for the re-oxygenation, demonstrating that the enzyme form $E_d^T$ rapidly binds to the oxygen but enters into a slow stage of the mechanism, and only when regenerated as $E_{ox}$ can enzymatic activity be obtained (Schemes 1BSM and 2B). Fig. 6 shows the $E_d^T$ re-oxygenation kinetics and the values of the apparent constant for transition at different pH values (Fig. 6 Inset). Note that at pH 6.5 the apparent constant is much higher, as occurs in the transition of $E_d^R$ to $E_d^T$ (Scheme 2B), which agrees with the explanation proposed in the previous step, indicating that the attraction between charges of opposing sign may contribute to the transition of $E_d^T$ to $E_d^R$ taking place rapidly and on a small scale.

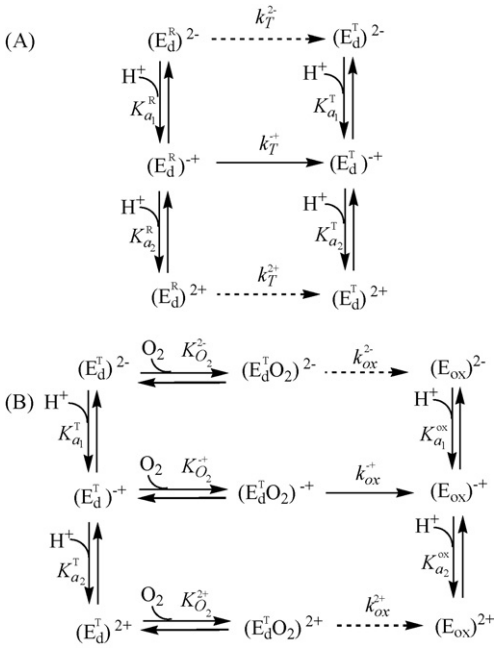


**Scheme 2.** (A) Effect of pH on the transition of $E_d^R$ to $E_d^T$, $K_{a_1}^R$, $K_{a_2}^R$, $K_{a_1}^T$ and $K_{a_2}^T$ are the corresponding deprotonation equilibrium constants and $k_T^{2-}$, $k_T^{+-}$ and $k_T^{2+}$ are the transition constants of the corresponding enzyme forms. (B) Effect of pH on the re-oxygenation of $E_d^T$. $K_{a_1}^T$ and $K_{a_2}^T$ have the same meaning as in Scheme 2A. $K_{a_1}^{ox}$ and $K_{a_2}^{ox}$ are the corresponding deprotonation constants. $K_{O_2}^{2-}$, $K_{O_2}^{+-}$ and $K_{O_2}^{2+}$ are the dissociation equilibrium constants of $(E_d^TO_2)^{2-}$, $(E_d^TO_2)^{+-}$ and $(E_d^TO_2)^{2+}$, respectively. $k_{ox}^{2-}$, $k_{ox}^{+-}$ and $k_{ox}^{2+}$ are the rate constants of the indicated transformations.

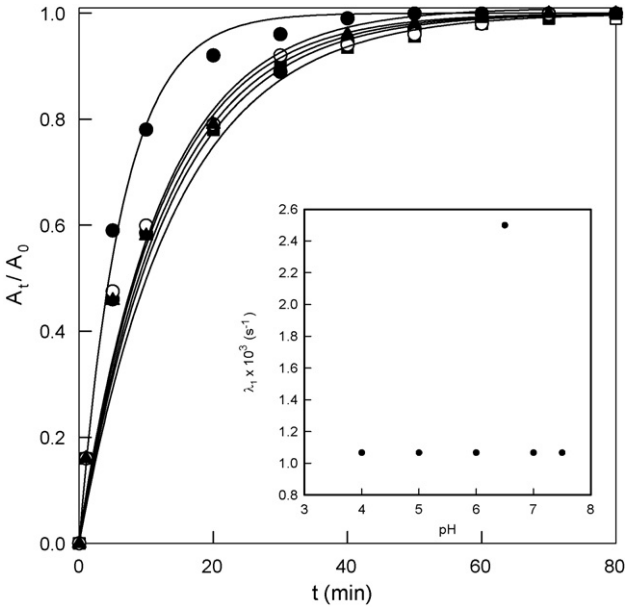


**Fig. 6.** Variation of the $A_t/A_0$-values *vs.* time obtained from a kinetic study of the effect of pH on the oxygenation of $E_d^T$ to $E_{ox}$. The form $E_d^T$ is generated in 1 mM sodium phosphate buffer (pH 7.0) and the oxygenation is studied at different pH values, mixing the enzyme $E_d^T$ on the oxygraph cell with 30 mM buffers. Taking aliquots at the indicated times, activity was determined with TBC (1 mM) and $O_2$ (0.26 mM). The buffers used were: 30 mM sodium phosphate buffer pH: ● 6.5, ○ 7.5, ■ 7.0, □ 6.0 and 30 mM sodium acetate buffer pH: ▲ 5.0, △ 4.0. Inset: Representation of apparent oxygenation constant $\lambda_1$ *vs.* pH.

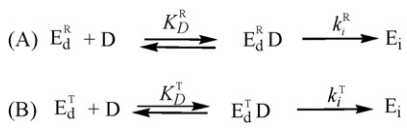


**Scheme 3.** (A) Kinetic mechanism of inactivation of $E_d^R$ by *o*-diphenol. (B) Kinetic mechanism of inactivation of $E_d^T$ by *o*-diphenol.

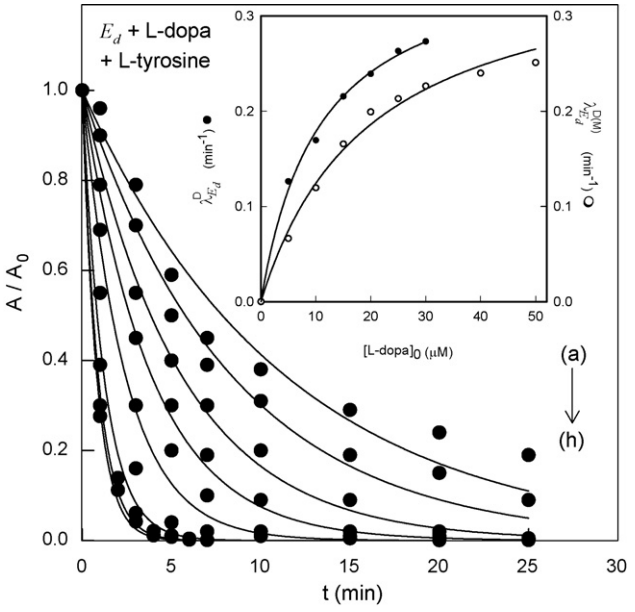


**Fig. 7.** Inactivation of the $E_d^R$ form of tyrosinase by *o*-diphenols. The form $E_d^R$ was obtained as is described in Section 2 and immediately incubated with *o*-diphenol (L-dopa), taking aliquots at different times to measure the residual activity with 2.5 mM L-dopa (λ = 475 nm). The values obtained were fitted to Eq. (6) and the apparent inactivation constant was obtained at each concentration of *o*-diphenol. The experimental conditions were: 30 mM sodium phosphate buffer (pH 7.0), 25 °C, $[E_d^R]_0 = 10$ nM (see Section 2), $[H_2O_2]_0 = 2$ μM and L-dopa (μM): (a) 5, (b) 10, (c) 15, (d) 20, (e) 25 and (f) 30. Inset. ● Representation of $\lambda^D_{E_d^R}$ *vs.* $[L\text{-dopa}]_0$. Fitting of these data to Eq. (8) gives the $K^D_{E_d^R}$. ○ Representation of the values of $\lambda^{D(M)}_{E_d^R}$ *vs.* $[L\text{-dopa}]_0$ obtained in the presence of L-tyrosine. Fitting to Eq. (10), gives the parameter $K^{D(M)}_{E_d^R}$ and analysis according to Eq. (12) gives $K^M_{E_d^R}$ (Table 2).

### 3.1.6. Incubations of $E_d^R$ and $E_d^T$ with *o*-diphenol

When the enzyme is pre-incubated with *o*-diphenol under aerobic conditions, both the recently generated $E_d^R$ (Scheme 3A) and $E_d^T$ (Scheme 3B) undergo a process of irreversible inactivation. The form $E_d^R$ shows a lower apparent binding constant (greater affinity) than $E_d^T$, although its apparent inactivation constant is slightly greater, indicating that its binding to the *o*-diphenol is favoured by the proximity of the copper atoms, which are probably further apart in $E_d^T$, hindering substrate binding, Fig. 7 and Table 2 (Scheme 3CSM). In the case of $E_d^T$ (Scheme 3B and Scheme 3DSM), inactivation also takes place. An analysis of the data of instantaneous activities *vs.* time, according to the following equations:

$$[E_a] = [E_d^R]_0\, e^{-\lambda^D_{E_d^R} t} \quad (6)$$

$$[E_a] = [E_d^T]_0\, e^{-\lambda^D_{E_d^T} t} \quad (7)$$

provides the apparent inactivation constants. A study of the different concentrations of *o*-diphenol and its analysis by Eqs. (8) and (9) give the values of $K^D_E$, $k^R_{i_D}$ and $k^T_{i_D}$ (Table 2).

$$\lambda^D_{E_d^R} = \frac{k^R_{i_D}[D]_0}{K^D_{E_d^R} + [D]_0} \quad (8)$$

$$\lambda^D_{E_d^T} = \frac{k^T_{i_D}[D]_0}{K^D_{E_d^T} + [D]_0} \quad (9)$$

In these cases (Schemes 3CSM and 3DSM), the *o*-diphenol could transfer the proton from the OH in *para*-position to the $His^{54}$ of the $Cu^A$ and the phenolate binds to the $Cu^A$, while the OH in *meta*-position later transfers its proton to the medium and binds in diaxial position. This binding will facilitate the oxidation/reduction and the enzyme is inactivated. Such a process may be favoured in $E_d^R$ compared with $E_d^T$ because of the proximity of the copper atoms.

The inactivation of the forms $E_d^R$ and $E_d^T$ with *o*-diphenol could have an industrial application in the agro-food industry for juice extraction since rapidly passing a nitrogen stream would lead to the formation of *deoxy*-tyrosinase, which, in the presence of the *o*-diphenols in the extracts (mainly chlorogenic acid), would lead to its inactivation, eliminating the enzymatic browning that normally occurs.

## 3.2. Monophenolase activity

### 3.2.1. Initial velocity measurements

From the measurements of initial velocity, it is possible to calculate the kinetic constants of the native enzyme and of the form $E_d^R$, which are shown in Table 1. When $E_d^T$ is formed, the kinetic properties with respect to L-tyrosine can be studied (see Table 1). Note the increase in $K_m^M$ and slight diminution of $V^M_{max}$, both of which agree with the results shown for the *o*-diphenols (Table 1). As mentioned above, by analogy with hemocyanin [8], the copper atoms are probably more distant in the form $E_d^T$ than in $E_d^R$ so that its affinity for the monophenol would be lower, despite the synergic effect observed between the substrates ($O_2$/L-tyrosine) as in the case of *o*-diphenols. The enzyme shows its characteristic lag, $\tau$, in these measurements.

### 3.2.2. Study of the transition of $E_d^R$ to $E_d^T$ by following the monophenolase activity with L-tyrosine

Under anaerobic conditions, $E_d^R$ is transformed into $E_d^T$, the enzymatic activity detected with L-tyrosine shows identical behaviour to that observed with the *o*-diphenol, TBC, and so the binding of the enzyme with the pair $O_2$/monophenol shows the same synergic effect as with the *o*-diphenol, Fig. 8. The values of the

**Table 2**
Equilibrium and kinetic constants for the inactivation of $E_d^T$ and $E_d^R$ by *o*-diphenols and its protection by monophenols.

| Enzymatic form | Substrate | $K^{Da}_E$ (μM) | $k^R_{i_D} \times 10^3$ (min$^{-1}$) | $k^T_{i_D} \times 10^3$ (min$^{-1}$) | $K^{Ma}_E$ (μM) |
|---|---|---|---|---|---|
| $E_d^T$ | L-dopa | 19.24 ± 2.12 | – | 0.25 ± 0.01 | – |
| | L-tyrosine | – | – | – | 22.32 ± 3.96 |
| $E_d^R$ | L-dopa | 10.77 ± 1.12 | 0.37 ± 0.01 | – | – |
| | L-tyrosine | – | – | – | 23.95 ± 2.99 |

[a] In $K^D_E$ and $K^M_E$, E corresponds to the enzymatic forms $E_d^T$ or $E_d^R$.

apparent transition constant are the same as those of Fig. 1 [$k_T = (6.5 \pm 0.5) \times 10^{-4}\ s^{-1}$]. The effect of pH (results not shown) is similar to that depicted in Fig. 5.

### 3.2.3. Re-oxygenation of $E_d^T$ and detection with monophenol

The form $E_d^T$ was generated and pre-incubated with oxygen. The kinetics was followed and the monophenolase activity was detected with L-tyrosine (Scheme 4ASM). Generation of the complex $E_{ox}M$ can follow the normal pathway, whereby the monophenol transfers the proton from OH in *para*-position to the peroxide, which acts as base, and the phenolate makes a nucleophilic attack on the $Cu^B$. This is followed by an electrophilic attack of the peroxide in the *meta*-position of the ring. This axial-equatorial bond must readjust before the concerted oxidation/reduction process can take place, as described in [47]. Fig. 8 Inset shows the results of this transition. Note that the apparent transition constant is the same as that obtained with *o*-diphenol [$\lambda_1 = (1.15 \pm 0.1) \times 10^{-3}\ s^{-1}$]. The effect of pH is similar to that depicted in Fig. 6 (results not shown). When the substrates (oxygen/monophenol) are added at the same time, enzymatic activity is generated, although to a lesser extent than for the native enzyme (Scheme 4BSM for $E_d^R$ and Scheme 4CSM for $E_d^T$). In this case, generation of the complex $E_{ox}M$ may partly follow any of the paths described in the corresponding schemes. Note that, as in the case of the *o*-diphenol (Scheme 1CSM), an atypical pathway of $E_{ox}M$ generation might exist, especially in the case of $E_d^T$ (Scheme 4CSM).

### 3.2.4. Study of the transition of $E_d^R$ to $E_d^T$ with sequential addition of substrates: first $O_2$ and then monophenol

Fig. 9 shows the results obtained. These are similar to the results in Fig. 3 with *o*-diphenol but also show the values of the lag phase, $\tau$. The explanation is also similar to that given for Fig. 3. At short pre-incubation times (1 min) with $O_2$, the form $E_d^R$ changes to $E_{ox}$ and enzymatic activity is favoured. The formation of $E_{ox}M$ would follow a normal pathway (Scheme 4BSM), $K_m^M$ is lower and so the $\tau$ is greater [34]. However, at longer times, there is more enzyme in the form $E_d^T$, and its binding with $O_2$ makes it follow the slow route, hindering enzymatic activity (Schemes 1ESM and 4CSM). The lag period in the tyrosinase mechanism increases when the concentration of enzyme decreases and when the enzyme affinity for the substrate increases (smaller $K_m$). These two situations are reflected in Fig. 9: at short times more enzyme exists in the $E_d^R$ form (smaller $K_m$ for L-tyrosine), and the lag is longer. At long times, more enzyme exists in the slow oxygenation pathway, less enzyme is totally active and so $\tau$ increases. These effects are amplified at short pre-incubation times with oxygen.

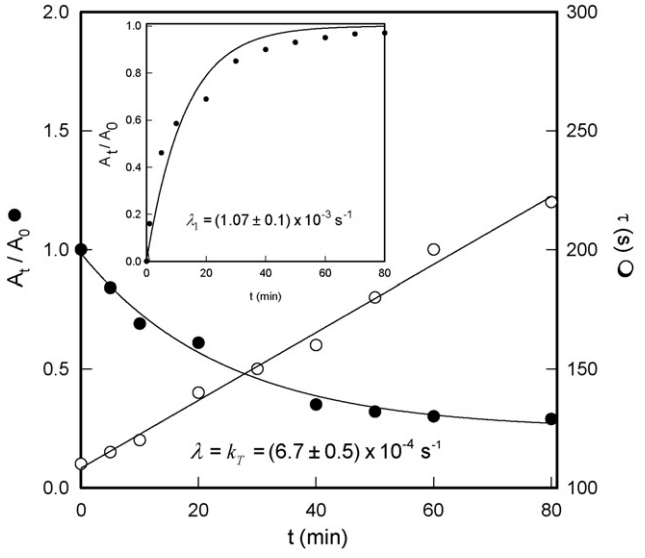


**Fig. 8.** Variation of the $A_t/A_0$-values *vs.* time obtained from a kinetic study of the transition of $E_d^R$ to $E_d^T$ followed by measuring monophenolase activity. The experimental conditions were: 30 mM sodium phosphate buffer (pH 7.0), 25 °C and $O_2$ (225 μM). The method was the same as in Fig. 1 but the instantaneous activities were measured with L-tyrosine (0.5 mM), spectrophotometrically measuring the increase in absorbance at 475 nm (●). Lag phase of monophenolase activity (○). Inset: Re-oxygenation of $E_d^T$ followed by monophenolase activity. Procedure as in Fig. 3, but activity followed as in above case (●).

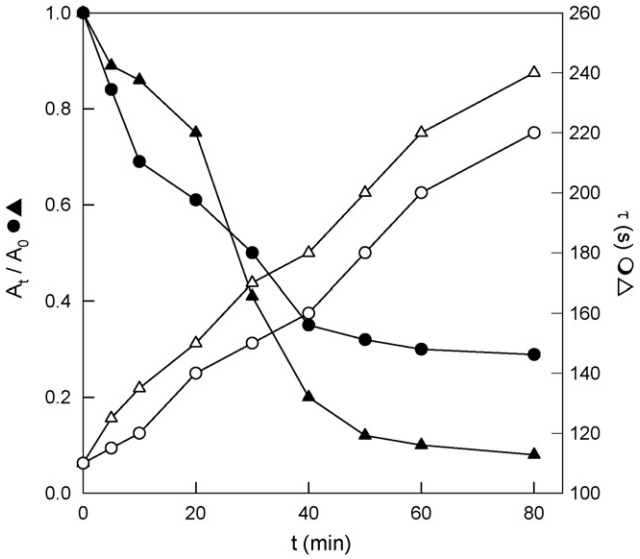


**Fig. 9.** Dependence of the $A_t/A_0$-values *vs.* time obtained from a kinetic study of the transition of $E_d^R$ to $E_d^T$ with sequential addition of substrates and followed through monophenolase activity. The method was the same as in Fig. 4 but the instantaneous activities were measured with L-tyrosine (0.5 mM), spectrophotometrically measuring the increase in absorbance at 475 nm. ● Instantaneous monophenolase activities without pre-incubating with $O_2$, ○ lag period ($\tau$) of the monophenolase activity without pre-incubating with $O_2$ ▲ Monophenolase activity, pre-incubating 1 min with $O_2$ (0.26 mM), △ lag phase ($\tau$) of monophenolase activity, pre-incubating 1 min with $O_2$ (0.26 mM).

### 3.2.5. Pre-incubation of the forms $E_d^R$ and $E_d^T$ with monophenols

When $E_d^R$ and $E_d^T$ are pre-incubated with small quantities of monophenol and the activity with *o*-diphenol is registered, no inactivation is detected (result not shown), although the monophenol binds to the enzyme, as can be seen from the fact that monophenol protects it from inactivation by *o*-diphenol (Fig. 7 for $E_d^R$; in the case of $E_d^T$, the results were similar) (Scheme 4A for $E_d^R$ and Scheme 4B

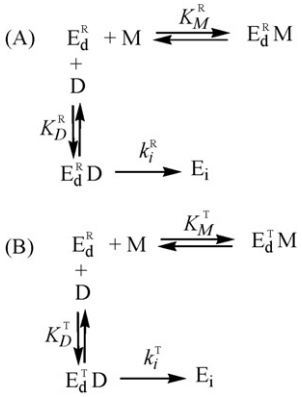


**Scheme 4.** (A) Kinetic mechanism to explain inactivation of $E_d^R$ by *o*-diphenol and its protection by monophenol. (B) Kinetic mechanism to explain inactivation of $E_d^T$ by *o*-diphenol and its protection by monophenol.

for $E_d^T$). A study of enzyme inactivation at different concentrations of *o*-diphenol in the presence of L-tyrosine (20 μM), provides the value of the apparent inactivation constant ($\lambda_{E_d^R}^{D(M)}$ or $\lambda_{E_d^T}^{D(M)}$, respectively) (result not shown), and an analysis by non-linear regression to Eqs. (10) and (11) provides the values of $K_{E_d^R}^{D(M)}$ and $K_{E_d^T}^{(M)}$ for $E_d^R$ and $E_d^R$, respectively.

$$\lambda_{E_d^R}^{D(M)} = \frac{k_{i_{D(M)}}^R [D]_0}{K_{E_d^R}^{D(M)} + [D]_0} \quad (10)$$

$$\lambda_{E_d^T}^{D(M)} = \frac{k_{i_{D(M)}}^T [D]_0}{K_{E_d^T}^{D(M)} + [D]_0} \quad (11)$$

where $\lambda_{E_d^R}^{D(M)}$ is the apparent inactivation constant of $E_d^R$ for L-dopa in the presence of L-tyrosine (see Fig. 7 Inset), $\lambda_{E_d^T}^{D(M)}$ is the apparent inactivation constant of $E_d^T$ for L-dopa in the presence of L-tyrosine, $k_{i_{D(M)}}^R$ is maximum value of $\lambda_{E_d^R}^{D(M)}$ for saturating substrate and $k_{i_{D(M)}}^T$ is maximum value of $\lambda_{E_d^T}^{D(M)}$ for saturating substrate (result not shown for $E_d^T$). From $K_{E_d^R}^{D(M)}$ and $K_{E_d^T}^{(M)}$ and according to Eqs. (12) and (13), we can calculate $K_{E_d^R}^{M}$ and $K_{E_d^T}^{M}$, the binding constants of L-tyrosine for $E_d^R$ and $E_d^T$, respectively.

$$K_{E_d^R}^{D(M)} = K_{E_d^R}^{D} \left(1 + \frac{[M]_0}{K_{E_d^R}^{M}}\right) \quad (12)$$

$$K_{E_d^T}^{D(M)} = K_{E_d^T}^{D} \left(1 + \frac{[M]_0}{K_{E_d^T}^{M}}\right) \quad (13)$$

When the transition of $E_d^R$ to $E_d^T$ was studied in the presence of 30 μM L-tyrosine, the kinetics was the same as in its absence (Fig. 8). Under anaerobic conditions, the most probable binding way of the monophenol to the $Cu^A$ would be through previous transfer the proton of OH in *para*-position to $His^{54}$, followed by the reversible attack of the phenolate on this $Cu^A$ (Schemes 5CMS and 5DMS for $E_d^R$ and $E_d^T$, respectively).

## 4. Conclusions

We have carried out a kinetic study of the *deoxy*-tyrosinase (intermediate in the tyrosinase catalytic cycle) obtained under anaerobic conditions from $E_{ox}$. The results obtained can be explained by the structural and energetic aspects demonstrated with *deoxy*-hemocyanin [8]. *Deoxy*-tyrosinase exists in two forms, $E_d^R$ (relaxed) and $E_d^T$ (tense), the latter being more stable. The pH affects the transition of $E_d^R$ to $E_d^T$: at values other than pH 6.5, the generation of two positive or negative charges may initiate the transition process, which will be slow both in the transition of $E_d^R$ to $E_d^T$ and in the re-oxygenation of $E_d^T$. However, at pH 6.5 the transition step, while being less pronounced, occurs more rapidly, and the properties of $E_d^T$ and of the native enzyme are practically the same. The kinetic properties of these enzymatic forms differ, especially as regards their binding affinity for their substrates, but not as regards their catalytic capacity. Under anaerobic conditions, the *o*-diphenols irreversibly inactivate the enzyme in both $E_d^R$ and $E_d^T$ forms, but the monophenols protect it from inactivation. This inactivation process may have industrial applications in, for example, the food industry since a nitrogen stream could be passed through a juice extract to obtain *deoxy*-tyrosinase. Since different *o*-diphenols would exist in this extract (mainly chlorogenic acid), this tyrosinase could be inactivated, thus diminishing considerably the enzymatic browning that normally occurs.

## Acknowledgements

This paper was partially supported by grants from the Ministerio de Educación y Ciencia (Madrid, Spain) Projects BIO2006-15363 and SAF2006-07040-C02-01, from the Fundación Séneca (CARM, Murcia, Spain) Project 00672/PI/04, from the Consejería de Educación (CARM, Murcia, Spain) BIO-BMC 06/01-0004, and from FISCAM PI-2007/53. JLMM has a fellowship from the Ministerio de Educación y Ciencia (Madrid, Spain) Reference AP2005-4721. FGM has a fellowship from Fundación Caja Murcia (Murcia, Spain).

## Appendix A.

Expression of the variation in enzymatic activity with time during the transition of $E_d^R$ to $E_d^T$ according to the following Scheme.$E_d^R \xrightarrow{k_T} E_d^T$

Variation of $E_d^R$ and $E_d^T$ with time:

$$[E_d^R]_t = [E_d^R]_0 \, e^{-k_T t} \quad (1A)$$

$$[E_d^T]_t = [E_d^R]_0 \, (1 - e^{-k_T t}) \quad (2A)$$

Variation in activity with time:

$$A_t = A_t^{E_d^R} + A_t^{E_d^T} \quad (3A)$$

or

$$V_0^t = V_0^{t(E_d^R)} + V_0^{t(E_d^T)} \quad (4A)$$

As regards initial activity:

$$\frac{A_t}{A_0} = \frac{A_t^{E_d^R} + A_t^{E_d^T}}{A_0} = \frac{V_0^t}{V_0} = \frac{V_0^{t(E_d^R)} + V_0^{t(E_d^T)}}{V_0} \quad (5A)$$

The expressions of $V_0^{t(E_d^R)}$, $V_0^{t(E_d^T)}$ and $V_0$ are:

$$V_0^{t(E_d^D)} = \frac{k_{cat}^R [E]_0 \, e^{-k_T t} [D]_0}{K_{m_D}^R + [D]_0} \quad (6A)$$

$$V_0^{t(E_d^T)} = \frac{k_{cat}^T [E]_0 (1 - e^{-k_T t}) [O_2]_0 [D]_0}{K_{O_2}^T K_{m_D}^T + K_{m_D}^T [O_2]_0 + K_{m_{O_2}}^T [D]_0 + [O_2]_0 [D]_0} \quad (7A)$$

$$V^{E_d^R} = \frac{k_{cat}^R [E]_0 [D]_0}{K_{m_D}^R + [D]_0} \quad (8A)$$

In agreement with Eq. (5A):

$$\frac{A_t}{A_0} = \frac{V_0^t}{V_0} = \alpha + \beta e^{-\lambda t} = \alpha + \beta e^{-k_T t} \quad (9A)$$

with

$$\alpha = \frac{k_{cat}^T (K_{m_D}^R + [D]_0)[O_2]_0}{k_{cat}^R (K_{O_2}^T K_{m_D}^T + K_{m_D}^T [O_2]_0 + K_{m_{O_2}}^T [D]_0 + [O_2]_0 [D]_0)} \quad (10A)$$

$$\beta = 1 - \alpha = 1 - \frac{k_{cat}^T (K_{m_D}^R + [D]_0)[O_2]_0}{k_{cat}^R (K_{O_2}^T K_{m_D}^T + K_{m_D}^T [O_2]_0 + K_{m_{O_2}}^T [D]_0 + [O_2]_0 [D]_0)} \quad (11A)$$

where $k_{cat}^R$ and $k_{cat}^T$ are the catalytic constant for $E_d^R$ and $E_d^T$ forms of tyrosinase, respectively; $K_{m_D}^R$ and $K_{m_D}^T$ are the Michaelis constants for the *o*-diphenol of the $E_d^R$ and $E_d^T$ forms of tyrosinase, respectively; $K_{O_2}^T$ is the dissociation constant for the oxygen of the $E_d^T$ form of

tyrosinase and $K^T_{m_{O_2}}$ is the Michaelis constant for the oxygen of the $E^T_d$ form of tyrosinase.

## Appendix B.

The $E^T_d$ oxygenation mechanism can be depicted as:

$$E^T_d + O_2 \underset{k_r}{\overset{k_b}{\rightleftarrows}} E^T_d O_2 \xrightarrow{k*} (E^T_d O_2)^* \xrightarrow{k_{ox}} E_{ox}$$

Variation in concentration of $E_{ox}$ with time, considering that the binding of $O_2$ in rapid equilibrium is:

$$[E_{ox}] = [E^T_d]_0 + A_1\, e^{-\lambda_1 t} + A_2\, e^{-\lambda_2 t} \tag{1B}$$

with

$$\lambda_1 = \frac{k^*[O_2]_0}{K^T_{O_2} + [O_2]_0} \tag{2B}$$

$$\lambda_2 = k_{ox} \tag{3B}$$

$$A_1 = \frac{k_{ox}(K^T_{O_2} + [O_2]_0)[E^T_d]_0}{k^*[O_2]_0 - k_{ox}(K^T_{O_2} + [O_2]_0)} \tag{4B}$$

$$A_2 = \frac{k^*[O_2]_0[E^T_d]_0}{k_{ox}(K^T_{O_2} + [O_2]_0) - k^*[O_2]_0} \tag{5B}$$

$$K^T_{O_2} = \frac{k_r}{k_b} \tag{6B}$$

If $\lambda_2 \gg \lambda_1$, then:

$$[E_{ox}] = [E^T_d]_0(1 - e^{-\lambda_1 t}) \tag{7B}$$

If $K^T_{O_2} \gg [O_2]_0$, then, from Eq. (2B):

$$\lambda_1 = \frac{k^*}{K^T_{O_2}}[O_2]_0 \tag{8B}$$

## Appendix C. Supplementary data

Supplementary data associated with this article can be found, in the online version, at doi:10.1016/j.molcatb.2009.10.005.

## References


[1] E.I. Solomon, U.M. Sundaram, T.E. Machonkin, Chem. Rev. 96 (1996) 2563–2606.
[2] A.C. Rosenzweig, M.H. Sazinsky, Curr. Opin. Struct. Biol. 16 (2006) 729–735.
[3] R.L. Jolley, L.H. Evans, N. Makino, H.S. Mason, J. Biol. Chem. 249 (1974) 335–345.
[4] M.E. Cuff, K.I. Miller, K.E. van Holde, W.A. Hendrickson, J. Mol. Biol. 278 (1998) 855–870.
[5] T. Klabunde, C. Eicken, J.C. Sacchettini, B. Krebs, Nat. Struct. Biol. 5 (1998) 1084–1090.
[6] Y. Matoba, T. Kumagai, A. Yamamoto, H. Yoshitsu, M. Sugiyama, J. Biol. Chem. 281 (2006) 8981–8990.
[7] M. Beltramini, L. Bubacco, B. Salvato, L. Casella, M. Gullotti, S. Garofani, Biochim. Biophys. Acta 1120 (1992) 24–32.
[8] M. Metz, E.I. Solomon, J. Am. Chem. Soc. 123 (2001) 4938–4950.
[9] E.I. Solomon, P. Chen, M. Metz, S.K. Lee, A.E. Palmer, Angew. Chem. Int. Ed. Engl. 40 (2001) 4570–4590.
[10] P. Chen, E.I. Solomon, Proc. Natl. Acad. Sci. U.S.A. 101 (2004) 13105–13110.
[11] W. Erker, R. Hübler, H. Decker, Biochim. Biophys. Acta 1780 (2008) 1143–1147.
[12] L. Ronda, S. Faggiano, S. Bettati, N. Hellmann, H. Decker, T. Weidenbach, A. Mozzarelli, Gene 398 (2007) 202–207.
[13] T.N. Sorrell, M. Beltramini, K. Lerch, J. Biol. Chem. 263 (1988) 9576–9577.
[14] S. Hirota, T. Kawahara, E. Lonardi, E. de Waal, N. Funasaki, G.W. Canters, J. Am. Chem. Soc. 127 (2005) 17966–17967.
[15] S. Della Longa, E.I. Ascone, A. Bianconi, A. Bonfigli, A. Castellano, O. Zarivi, M. Miranda, J. Biol. Chem. 271 (1996) 21025–21030.
[16] H. Decker, T. Schweikardt, D. Nillius, U. Salzbrunn, E. Jaenicke, F. Tuczek, Gene 398 (2007) 183–191.
[17] H. Decker, F. Tuczek, Trends Biochem. Sci. 25 (2000) 392–397.
[18] L. Bubacco, M. van Gastel, M. Benfatto, A.W. Tepper, G.W. Canters, Micron 35 (2004) 143–145.
[19] B. Salvato, M. Santamaria, M. Beltramini, G. Alzuet, L. Casella, Biochemistry 37 (1998) 14065–14077.
[20] E. Jaenicke, H. Decker, FEBS J. 275 (2008) 1518–1528.
[21] D. Nillius, E. Jaenicke, H. Decker, FEBS Lett. 582 (2008) 749–754.
[22] S. Baird, S.M. Kelly, N.C. Price, E. Jaenicke, C. Meesters, D. Nillius, H. Decker, J. Nairn, Biochim. Biophys. Acta 1774 (2007) 1380–1394.
[23] H. Decker, E. Jaenicke, Dev. Comp. Immunol. 28 (2004) 673–687.
[24] E. Jaenicke, H. Decker, Micron 35 (2004) 89–90.
[25] H. Decker, M. Ryan, E. Jaenicke, N. Terwilliger, J. Biol. Chem. 276 (2001) 17796–17799.
[26] H. Decker, T. Rimke, J. Biol. Chem. 273 (1998) 25889–25892.
[27] K. Suzuki, C. Shimokawa, C. Morioka, S. Itoh, Biochemistry 47 (2008) 7108–7115.
[28] L.M. Mirica, D.J. Rudd, M.A. Vance, E.I. Solomon, K.O. Hodgson, B. Hedman, T. Stack, J. Am. Chem. Soc. 128 (2006) 2654–2665.
[29] L.M. Mirica, M. Vance, D.J. Rudd, B. Hedman, K.O. Hodgson, E.I. Solomon, T.D. Stack, Science 308 (2005) 1890–1892.
[30] O. Sander, A. Henss, C. Näther, C. Würtele, M. Holthausen, S. Schindler, F. Tuczek, Chemistry 14 (2008) 9714–9729.
[31] J.N. Rodriguez-Lopez, J. Tudela, R. Varon, F. Garcia-Carmona, F. Garcia-Canovas, J. Biol. Chem. 267 (1992) 3801–3810.
[32] J.N. Rodriguez-Lopez, L.G. Fenoll, P.A. Garcia-Ruiz, R. Varon, J. Tudela, R.N. Thorneley, F. Garcia-Canovas, Biochemistry 39 (2000) 10497–10506.
[33] L.G. Fenoll, J.N. Rodriguez-Lopez, F. Garcia-Sevilla, P.A. Garcia-Ruiz, R. Varon, F. Garcia-Canovas, J. Tudela, Biochim. Biophys. Acta 1548 (2001) 1–22.
[34] F.G. Molina, J.L. Munoz, R. Varon, J.N. Rodriguez-Lopez, F.G. Canovas, J. Tudela, Int. J. Biochem. Cell Biol. 39 (2007) 238–252.
[35] J.L. Muñoz-Muñoz, F. Garcia-Molina, P.A. Garcia-Ruiz, M. Molina-Alarcón, J. Tudela, F. Garcia-Canovas, J.N. Rodriguez-Lopez, Biochem. J. 416 (2008) 431–440.
[36] J.L. Muñoz-Muñoz, F. Garcia-Molina, P.A. Garcia-Ruiz, R. Varon, J. Tudela, F. Garcia-Canovas, J.N. Rodriguez-Lopez, Biochim. Biophys. Acta 1794 (2009) 244–253.
[37] M.M. Bradford, Anal. Biochem. 7 (1976) 248–254.
[38] J.N. Rodriguez-Lopez, J.R. Ros-Martinez, R. Varon, F. Garcia-Canovas, Anal. Biochem. 202 (1992) 356–360.
[39] J.L. Munoz, F. Garcia-Molina, R. Varon, J.N. Rodriguez-Lopez, F. Garcia-Canovas, J. Tudela, Anal. Biochem. 351 (2006) 128–138.
[40] M. Jackman, M. Huber, A. Hajnal, K. Lerch, Biochem. J. 282 (1992) 915–918.
[41] R. Aasa, J. Deinum, K. Lerch, B. Reinhammar, Biochim. Biophys. Acta 535 (1978) 287–298.
[42] Jandel Scientific, Sigma Plot 9.0 for Windows™, Jandel Scientific, Core Madera, 2006.
[43] J.R. Ros, J.N. Rodriguez-Lopez, F. Garcia-Canovas, Biochim. Biophys. Acta 1204 (1994) 33–42.
[44] J.C. Espin, P.A. Garcia-Ruiz, J. Tudela, F. Garcia-Canovas, Biochem. J. 331 (1998) 547–551.
[45] J.C. Espin, R. Varon, L.G. Fenoll, M.A. Gilabert, P.A. Garcia-Ruiz, J. Tudela, F. Garcia-Canovas, Eur. J. Biochem. 267 (2000) 1270–1279.
[46] J. Yoon, S. Fujii, E.I. Solomon, Proc. Natl. Acad. Sci. U.S.A. 106 (2009) 6585–6590.
[47] J.N. Rodriguez-Lopez, L.G. Fenoll, M.J. Peñalver, P.A. Garcia-Ruiz, R. Varon, F. Martinez-Ortiz, F. Garcia-Canovas, J. Tudela, Biochim. Biophys. Acta 1548 (2001) 238–256.